Enhanced Design and Electromagnetic Analysis of Synchronous Reluctance Machines Using Multi-Material Additive Manufacturing

Siddique Akbar
Profluxx GmbH
Ingolstadt, Germany
siddique.akbar@profluxx.com

Yitbarek Tedla Bekele
Leibniz University Hannover
Institute of Drives and Power Electronics
Hannover, Germany
Yitbarek.bekele@ial.uni-hannover.de

Amir Ebrahimi
University of Bremen
Institute of Electrical Drives, Power Electronics and Devices
Bremen, Germany
ebrahimi@ialb.uni-bremen.de

Bernd Ponick
Leibniz University Hanover
Institute for Drives and Power Electronics
Hannover, Germany
ponick@ial.uni-hannover.de

***Abstract*— This article comprehensively investigates the design and simulation of synchronous reluctance machines (SynRMs) using multi-material additive manufacturing (MMAM) methods. The main goal is to improve the electromagnetic performance of the machine by strategically utilizing various materials in the rotor's edge bridges to reduce quadrature inductance L_q. A comparative analysis is led on various combinations of magnetic and non-magnetic materials, examining conventionally built machines with single materials alongside additively manufactured machines with both single and multiple materials. A demonstrator machine is built to analyze and determine essential performance parameters, emphasizing the optimization of the rotor. The research establishes an optimized rotor model to enhance electromagnetic performance and examines the operational impacts on electromagnetic torque and torque oscillations. Analytical and simulation findings illustrate the capability of multi-material additive manufacturing to improve the performance of conventional electric machines.**

Keywords*— *Additive manufacturing, multi materials, genetic algorithm, synchronous reluctance machine.

I. Introduction

Additive manufacturing (AM) technology offers new design options for electric machines by overcoming the limitations of conventional motor production methods. AM fabricates components by employing a process that builds up material layer upon layer, which minimizes material wastage and allows for the creation of complex motor parts with improved 3D design flexibility [1].

In recent years, there has been a push to design electric machines that do not rely on expensive and environmentally harmful rare-earth permanent magnet (PM) materials. Among these alternatives, SynRMs have gained popularity due to their simple, robust design that requires no rotor windings and no PMs, thus eliminating demagnetization risks and copper loss in the rotor while reducing cooling requirements [2].

AM is considered as an interesting alternative to the well-established methods for producing magnetic parts and components. While there is a great deal of research on this topic, AM has effectively produced single-material components for electric machines, yet multi-material additive manufacturing (MMAM) signifies an emerging innovation, though still in its early stages. This technology facilitates the combination of different materials into a single component that meets both structural and functional requirements, thus potentially improving motor performance by directing magnetic flux, minimizing flux leakage, and strategically positioning conductive materials in the rotor to improve torque density [1, 3].

This section touches on a few noteworthy pieces of research. In the study conducted in [3], the primary focus was on AM of different parts of the SynRM, with only limited information regarding the improvements in machine performance. An improved electromagnetic design was built in [4] with a conical air gap and a 3D flux path which results in twice the power density compared to the base design. In [5], an additively manufactured FeSi6.7 stator with a Hilbert shape reduced eddy current losses, enhancing torque density by 4.5%. Literature indicates a low technological maturity in AM for electric machines. [6] highlights MMAM's potential for SynRM rotors by layering magnetic and non-magnetic materials, improving structural integrity, enabling higher speeds, and achieving up to 4x power density over conventional designs.

In this work, a novel design utilizing MMAM is presented for the SynRM rotor, focusing on enhancing torque density and reducing the quadrature inductance L_q. While the design follows a layer-by-layer fabrication process, it innovatively incorporates non-magnetic materials at specific locations within the rotor. This selective placement is tailored to improve magnetic flux guidance and suppress leakage. Extensive simulations across various material combinations validate the effectiveness of this advanced MMAM design, establishing new standards for torque density enhancement in SynRMs. To the best of the authors' knowledge, except for reference [6], no other data on the MMAM-based design of SynRMs is currently available, highlighting the significance of this contribution to the field.

This paper is organized as follows: Section II presents the output equations and inductance calculations, providing the fundamental expressions governing the machine's performance. Section III details the electromagnetic analysis to identify the best-performing design. Section IV focuses on

the optimization process, where material selection and structural refinements are explored to enhance the machine's electromagnetic properties. Section V covers the efficiency mapping and loss analysis of the optimized design, evaluating its operational effectiveness and performance trade-offs. Finally, Section VI concludes the study, summarizing the key findings and highlighting directions for improving the viability of additively manufactured Synchronous Reluctance Machines (AM-SynRM).

II. OPERATING PRINCIPLES AND OUTPUT EQUATIONS

SynRMs have two rotor axes: the q-axis and the d-axis, as shown in Fig.1. When current flows through the stator's three-phase winding, it creates a magnetic field that the rotor aligns with by rotating its d-axis toward the field to minimize reluctance. The difference in reluctance between the q-axis and d-axis generates torque, with torque magnitude being directly proportional to the reluctance difference. The voltage equations of SynRMs are given by [7].

$$u_{\mathrm{d}} = R_{\mathrm{s}} i_{\mathrm{d}} + (\mathrm{d}\Psi_{\mathrm{d}} / \mathrm{d}t) - \omega \Psi_{\mathrm{q}} \quad (1)$$

$$u_{\mathrm{q}} = R_{\mathrm{s}} i_{\mathrm{q}} + \left(\mathrm{d}\Psi_{\mathrm{q}} / \mathrm{d}t\right) + \omega \Psi_{\mathrm{d}} \quad (2)$$

In (1) and (2), R_{s} representing the winding resistance, u_d, u_q , i_{d} and i_{q} denoting voltage and current on the d- and q-axes, respectively, Ψ_d and Ψ_q representing flux linkages on the d- and q-axes. While the angular frequency of the stator voltage and current are represented by ω.

Similarly, L_{d} and L_{q} can be calculated as

$$L_{\mathrm{d}} = \Psi_{\mathrm{d}} / i_{\mathrm{d}} \quad (3)$$

$$L_{\mathrm{q}} = \Psi_{\mathrm{q}} / i_{\mathrm{q}} \quad (4)$$

SynRM relies on the rotor saliency ratio ξ as a critical metric for rotor anisotropy characterization. It is defined as

$$\xi = L_{\mathrm{d}} / L_{\mathrm{q}} \quad (5)$$

The simplified torque in a SynRM can be calculated as

$$T = \frac{3}{2} p \left(L_{\mathrm{d}} - L_{\mathrm{q}}\right) i_{\mathrm{d}} i_{\mathrm{q}} \quad (6)$$

III. ELECTROMAGNETIC ANALYSIS

The electromagnetic analysis workflow, illustrated in Fig. 2, begins with the evaluation of a demonstrator SynRM, built using the traditional laminated manufacturing process shown in Fig. 3(a) To explore advanced manufacturing techniques, the same machine is then constructed using AM with a multi-material radially laminated structure, where one part consists of a conducting material and the other part of a non-conducting material, visually distinguished by gray and red colors Fig. 3(b). Further, an initial MMAM SynRM, incorporating multi-materials at specific locations such as rotor edges and bridges, is designed in Fig. 3(c).

Based on initial performance results, a comparative electromagnetic analysis of all these machine configurations is conducted. The most promising machine selected based on preliminary assessments is then further optimized, leading to

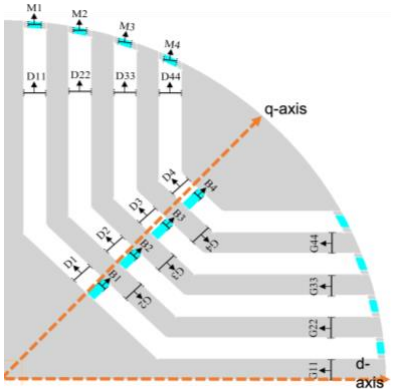

Fig. 1 Demonstrator SynRm with optimization variables

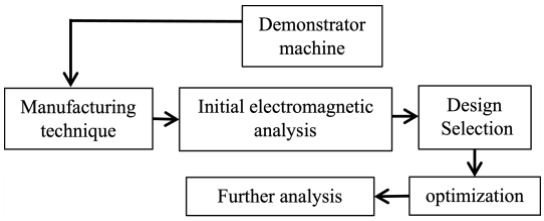

Fig. 2 Work flow

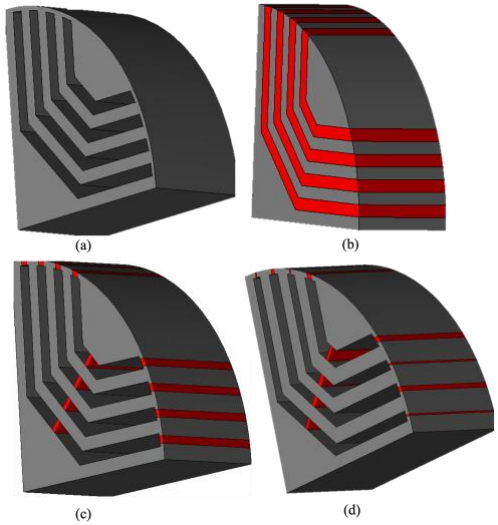

Fig. 3 Geometrical design of demonstrator machines: (a) conventional rotor (b) radially laminated AM rotor (c) initial MMAM rotor (d) optimized MMAM rotor

the final optimized MMAM machine Fig. 3(d). This optimized design is subjected to additional analysis with different multi-material configurations and undergoes a comprehensive electromagnetic assessment to validate performance improvements.

In this workflow, the electromagnetic analysis of the demonstrator SynRM, based on an industrial design, is presented in Table 1. The stator geometry remains fixed, while the rotor is designed for MMAM. Key parameters (Table 1) were analyzed using JMAG, starting with a conventional laminated steel design, followed by single-material configurations (FeSi, FeCo) and a multi-material approach incorporating FeCo and stainless steel 316L. The design was then optimized to maximize torque density and minimize torque oscillation using JMAG's optimization tools. The final optimized design, selected through this

systematic workflow, demonstrates improved performance and efficiency, confirming the benefits of multi-material additive manufacturing in SynRM development. The electromagnetic analysis workflow is illustrated in Fig.2.
The electromagnetic behavior of all these machines is compared systematically, and based on the preliminary performance assessment, the most promising machine is selected for optimization. This optimized design is further analyzed with different multi-material configurations, followed by a complete electromagnetic assessment for validation of the performance improvement.

A. Torque performance

Fig.4 compares the torque characteristics of demonstrator machines manufactured using different techniques. The analysis is based on the reluctance torque discussed in (6) , where torque depends on the current components and their alignment with the rotor's anisotropic inductance profile. The results show that the initial MMAM SynRM achieves the highest torque, followed by the conventional machine, while the radially laminated machine produces the lowest torque. The torque curve emphasizes the critical role of the current angle θ (angle between stator current and d-axis of rotor magnetic field) in torque generation. The analysis also helps in identifying the optimum current angle for each machine, ensuring maximum torque production. This highlights the importance of current angle optimization in SynRM control and design strategies.

B. Inductance calculation

Torque generation is governed by equation (6), where the difference between d-axis and q-axis inductances $(L_{\mathrm{d}} - L_{\mathrm{q}})$ making inductance characteristics a key performance indicator. Fig.5 shows that the initial MM Machine maintains a high L_{d} and lower L_{q} comparable to the conventional machine and the radially laminated AM machine.

C. Machine selection

Based on the electromagnetic performance analysis, the demonstrator machines designed using different manafacturing techniques exhibit varying torque characteristics. The results indicate that the initial MMAM SynRM outperforms the other configurations by achieving the highest torque.

Furthermore, the findings reveal that the initial MM machine maintains a high L_{d} and lower L_{q} , making it a more efficient choice compared to the conventional and radially laminated AM machines. Given these observations, the initial MMAM SynRM is the most promising candidate for further analysis due to its superior torque performance and favorable inductance characteristics.

IV. Optimization

A built-in genetic optimization algorithm in JMAG was employed to optimize the design of the demonstrator machine. This algorithm systematically adjusts key design parameters to enhance machine performance metrics like torque and torque oscillations. By simulating multiple iterations and refining the design through an evolutionary process, the optimization ensures that the demonstrator machine achieves optimal electromagnetic performance with

TABLE 1: GEOMETRICAL AND DESIGN DETAILS OF DEMONSTRATOR SYNRM.

Number of Poles	4	Yoke height	12.5 mm
Number of Slots	36	Rotor outer radius	42.7 mm
Stack length	110 mm	Slot area	55 mm2
Stator outer radius	70 mm	Number of conductors/slot	47
Stator inner radius	49 mm	Rated speed	1500 min^{-1}
Air gap	0.3 mm	Rated current	3.46 A

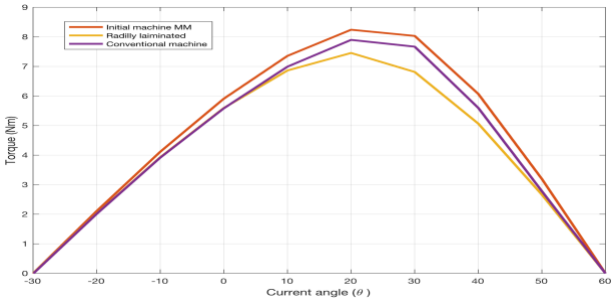

Fig. 4 Torque w.r.t different current angle

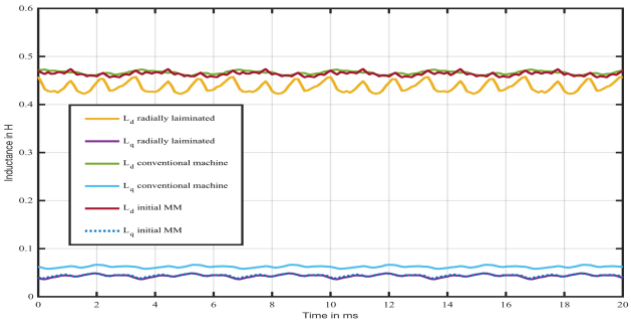

Fig. 5 d-q inductance calculation

minimal manual intervention. This approach accelerates the design process and enables effective exploration of complex parameter spaces. To enhance the rotor design of the demonstrator machine optimization process considers 23 key variables that significantly influence the machine's electromagnetic performance. These parameters are adjusted within predetermined limits, and their lowest, maximum, initial, and optimum values are presented in a related Table 2, while their positions in the design space are visually depicted in Fig.1. The objective function of optimization is set as

$$\max\ (T_{\mathrm{avg}})$$
$$\min\ (T_{\mathrm{oscillation}})$$

constraints

$$\begin{cases} T_{\mathrm{oscillatoin}} < \text{initial oscillation in torque} \\ T_{\mathrm{avg}} > \text{initail average torque} \end{cases}$$

Optimization Configuration:
Generations: 15
The population size is 30.
Total number of children: 29
Stopping criteria: 8
Step size: 2

The selected number of generations and population size offer a comprehensive examination of the design space. In contrast, the step size and stopping criteria are adjusted to

TABLE 2: PARAMETERS INVOLVED IN OPTIMIZATION

Symbol	Initial Value (mm)	Range (mm)	Optimum value (mm)
B1	0.5	0.3–1	0.387
B2	0.5	0.3–1	0.553
B3	0.5	0.3–1	0.545
B4	0.5	0.3–1	0.381
D1	2.5	1.5–3.3	2.232
D2	2.5	1.5–3.3	2.070
D3	2.5	1.5 –3.3	2.207
D4	2.5	1.5 –3.3	3.057
D11	2.5	2.1–3.3	2.215
D22	2.5	2.1–3.3	2.750
D33	2.5	2.1–3.3	2.167
D44	2.5	2.1–3.3	2.951
G2	2.5	1.5–3.3	2.740
G3	2.5	1.5–3.3	2.462
G4	2.5	1.5–3.3	3.215
G11	2.5	1.5–3.3	2.500
G22	2.5	1.5–3.3	2.952
G33	2.5	1.5–3.3	2.917
G44	2.5	1.5–3.3	3.044
M1	0.5	0.3–1.3	0.348
M2	0.5	0.3–1.3	0.972
M3	0.5	0.3–1.3	0.390
M4	0.5	0.3–1.3	1.174

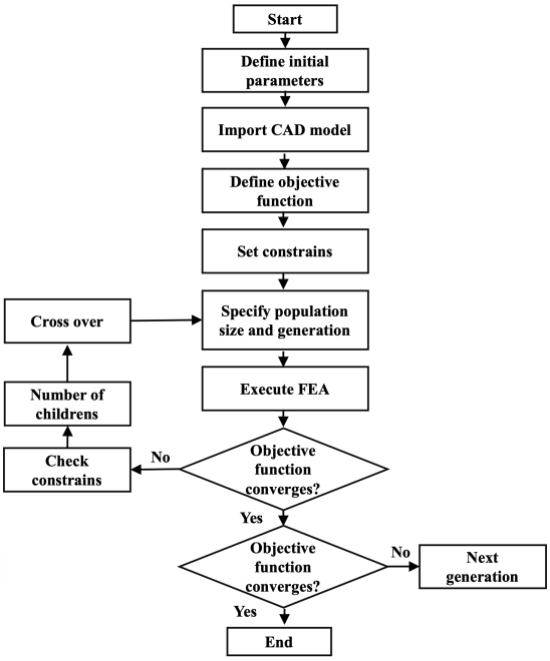

Fig. 6 Genetic algorithm workflow

achieve a balance calculating efficiency and optimization accuracy. The genetic algorithm follows a systematic procedure, as depicted in Fig.6. During the optimization process, the genetic algorithm gradually approaches an optimal rotor design by continuously improving the values of the parameters. The stopping criteria evaluate when the algorithm has reached an optimal design, ensuring that additional iterations will result in minimal improvements. The optimization of the bridge dimensions shows the sensitive balance between attaining high torque and lowering torque oscillations in the demonstrator machine. The best values for each bridge depend upon the intended operational features. However, in general, a distinct trade-off exists between torque and torque oscillations.

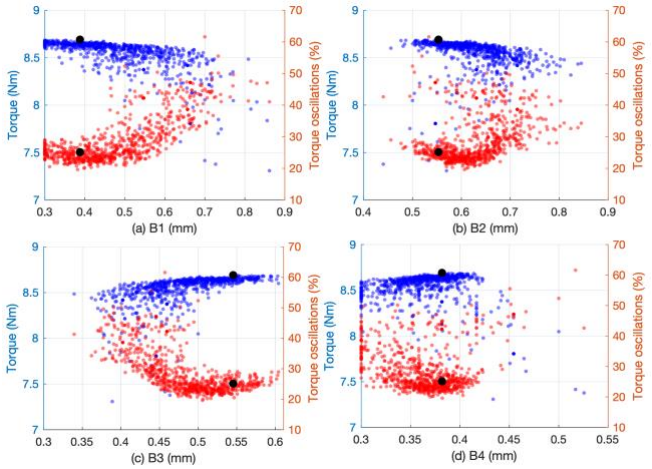

Fig. 7 Torque and torque oscillation w.r.t B1, B2,B3 and B4

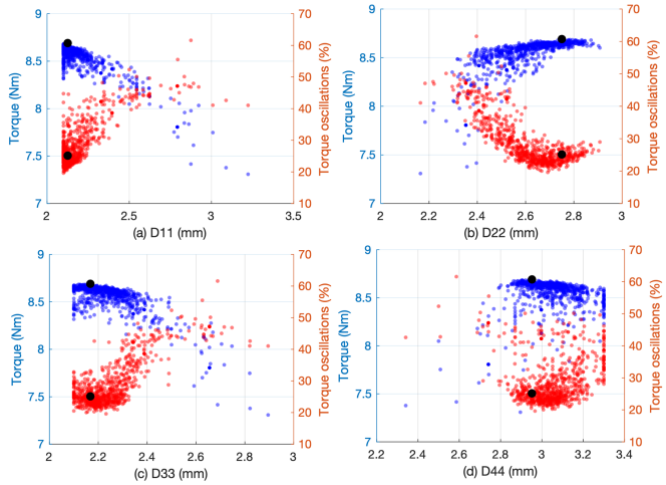

Fig. 8 Torque and torque oscillation w.r.t D11, D22, D33 and D44

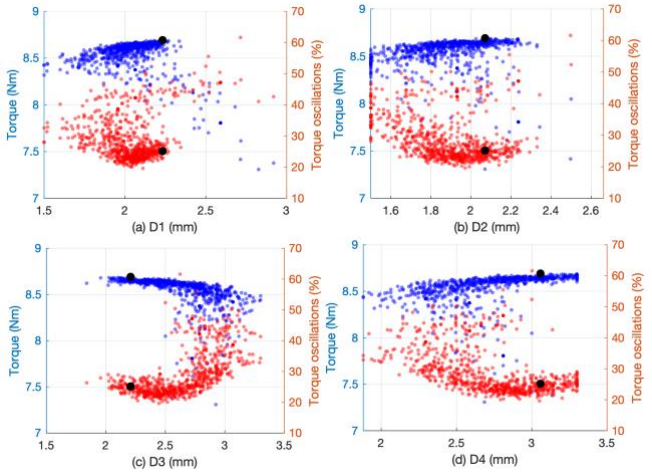

Fig.9 Torque and torque oscillation w.r.t D1, D2, D3 and D4

The figures offer a detailed representation of how each dimension of the bridge impacts the critical performance parameters, assisting in selecting the optimal configuration. The optimal value of these bridges is shown in Fig. 7(a-d) by black dots.

Fig. 8(a-d) and 9 (a-d) demonstrate the optimization outcomes for the widths of various sections of barriers in the

rotor. These barriers play a crucial role in determining the paths of magnetic flux and have a considerable impact on the machine's performance, especially in terms of torque production and torque oscillations. Each graphic depicts the correlation between a particular barrier width and the corresponding torque and oscillation rate.

Fig.10(a) illustrates all cases of the GA for the demonstrator MMAM SynRM. The x-axis represents the number of cases analyzed during the optimization process, the y-axis display average torque and torque oscillation across these cases. The figure clearly demonstrates the convergence characteristics of the genetic optimization process. The reliability of the optimization process in determining the best rotor design configuration for the SynRM is shown by the convergence to stable values after multiple iteration.

Moreover Fig. 10(b-d) and Fig. 11(a-d) show the optimization of gap arrangements in barriers of the demonstrator machine. The existence of these gaps directly impacts the distribution of magnetic flux, which in turn affects the torque and torque oscillation. The analysis illustrates an optimum range for each gap where torque is maximized and oscillations are minimized. Performance weakens outside of these suitable limits, resulting in higher oscillations and reduced torque.

Fig. 12 (a-d) represents the optimization results for the edge bridges near the outer surface of the rotor. These edge bridges, denoted as M1, M2, M3, and M4, are made of non-magnetic materials. The optimization aimed to determine the optimal dimensions for these bridges to enhance performance, mainly focusing on torque and its oscillations.

V. Efficiency Mapping and Losses of Optimized Design

The electromagnetic performance evaluation of MMAM SynRM is systematically analyzed through torque-speed characteristics, loss distribution, efficiency mapping, and power-torque relationships. Fig.13 illustrates the stator iron losses (W) as a function of torque and speed, showing a significant rise beyond speed 2000 min^{-1}, attributed to increased hysteresis effects and eddy currents within the bulk material, as AM-SynRM lacks traditional laminated core structures. Fig. 14 represents the rotor iron loss distribution, showing that while eddy losses remain moderate at medium speeds, they increase significantly at higher speeds >3000 min^{-1}, peaking at ~100 W. Unlike conventional machines where laminations suppress eddy losses, in AM-SynRM, these losses can be minimized by some advanced techniques [8]. Table.3 shows comparison of rotor iron losses in different machines geometries. Fig.15 maps the efficiency profile, revealing that efficiency remains above 85% in the medium-speed and mid-torque region, but declines in low-speed regions due to copper losses and at high speeds due to iron losses, emphasizing the importance of material property optimization and advanced control strategies for AM-SynRM. Fig. 16 presents the torque and power-speed characteristics, where torque remains nearly constant up to the base speed 1500 min^{-1} before decreasing due to field weakening, while power exhibits a linear increase, peaking at ~1200 W before saturation, dictated by the machine's voltage

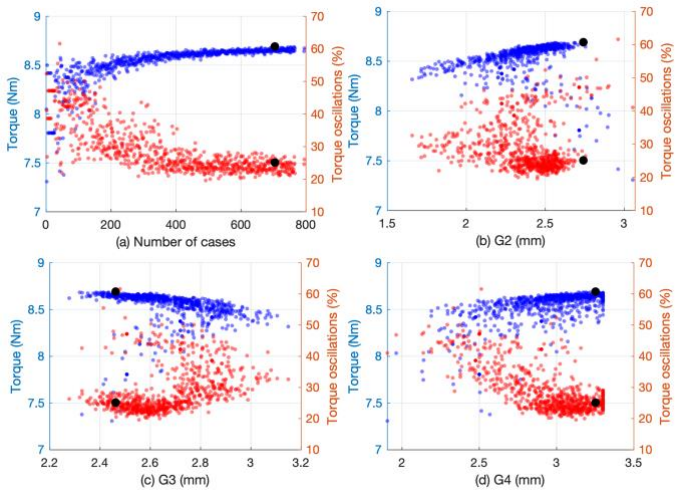

Fig. 10 Torque and torque oscillation w.r.t no of cases and G2, G3 and G4

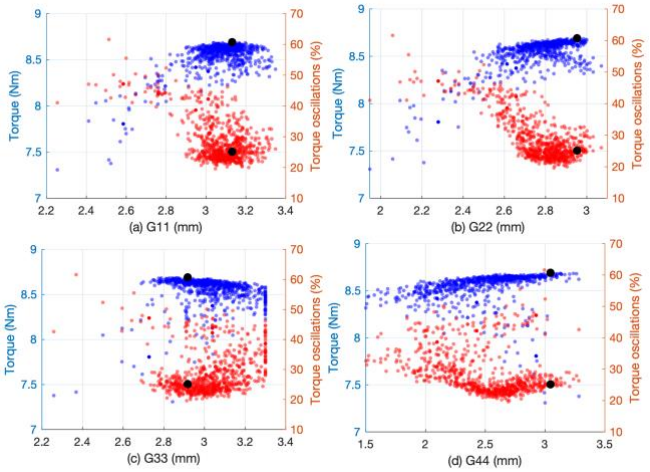

Fig. 11 Torque and torque oscillation w.r.t G11, G22, G33 and G44

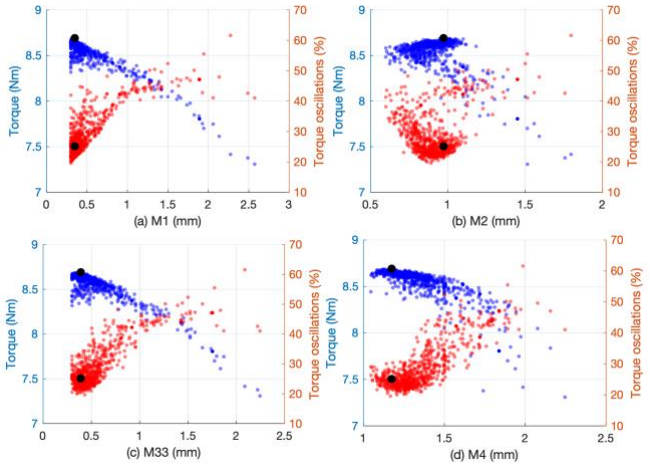

Fig. 12 Torque and torque oscillation w.r.t M1, M2, M3 and M4

constraints. These findings highlight the potential of AM in revolutionizing electric machine manufacturing by enabling complex geometries, tailored magnetic properties, and loss optimized, enhanced performance and efficiency in next-generation AM-SynRM applications.

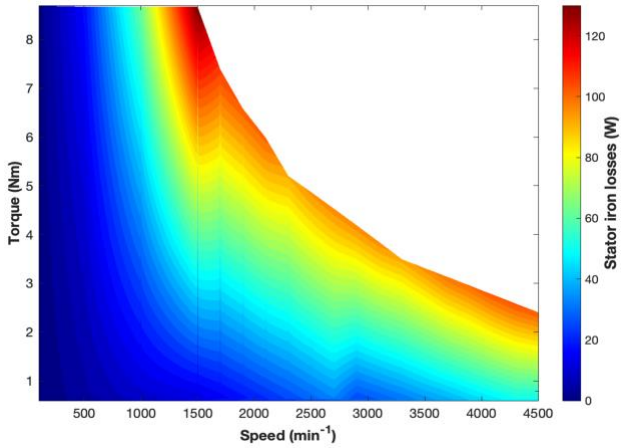

Fig. 13 Torque and iron losses w.r.t speed

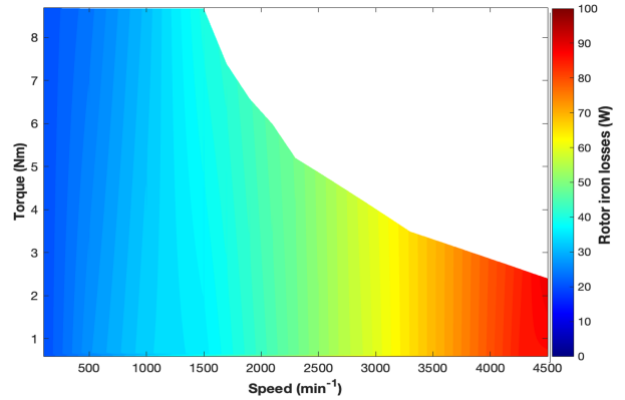

Fig. 14 Torque and eddy losses w.r.t speed

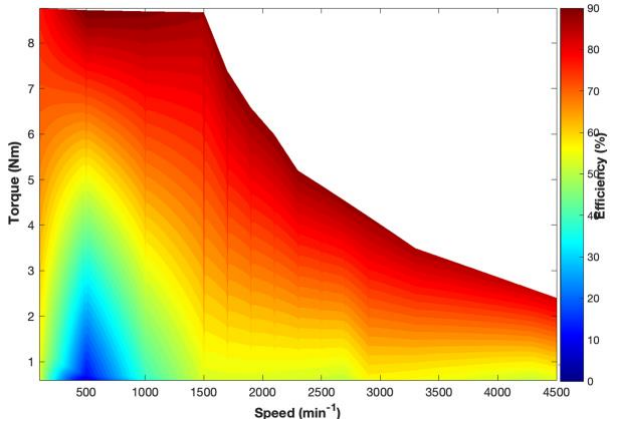

Fig. 15 Torque and efficiency w.r.t speed

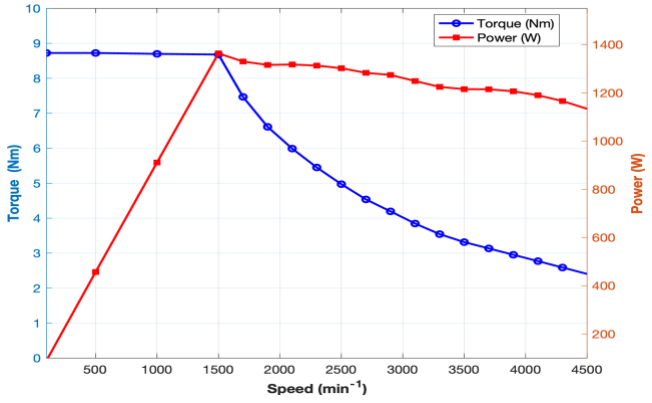

Fig. 16 Torque and power w.r.t speed

TABLE 3: PERFORMANCE COMPARISON OF DIFFERENT TOPOLOGIES

	Conventional machine	**Radially AM**	**Initial MM**	**Optimized MM**
Torque (Nm)	7.45	7.24	7.90	8.68
Oscillation (%)	27	60	40	25
Stator iron losses (W)	165.59	174.11	150	132
Rotor iron losses (W)	20	75	58	40
Output power (kW)	1.17	1.13	1.24	1.36
Efficiency	83.5	79	83	86
Power factor	0.75	0.70	0.79	0.79

VI. CONCLUSION

This study demonstrates the potential of multi-material additive manufacturing (MMAM) in improving the performance of synchronous reluctance machines (SynRMs). By strategically incorporating magnetic and non-magnetic materials within the rotor, this work achieves reduced L_q, and increased torque output. Through detailed electromagnetic analysis, the optimized multi-material design is shown to provide superior performance compared to conventional and single-material designs, achieving higher torque density. The findings underscore the effectiveness of MMAM in establishing new benchmarks in SynRM torque production

ACKNOWLEDGMENT

This research was supported by the European Union under the Marie Sklodowska-Curie Doctoral-Industrial project (HORIZON-MSCA-2021-DN001), EMByAM

Funded by the European Union

REFERENCES

[1] Tiismus, H., Kallaste, A., Naseer, M. U., Vaimann, T., and Rassõlkin, A., "Design and performance of laser additively manufactured core induction motor," *IEEE Access*, vol. 10, pp. 50137-50152, 2022. doi: 10.1109/ACCESS.2022.DOI

[2] S. Zhang, C. Liu, S. Wang, Y. Wang and J. Zhu, "Preliminary Design and Comparative Analysis of a New Synchronous Reluctance Machine With Hybrid Cores," in IEEE Transactions on Magnetics, vol. 59, no. 11, pp. 1-5, Nov. 2023, Art no. 8103205, doi: 10.1109/TMAG.2023.3293799.

[3] Z. Y. Zhang, K. J. Jhong, C. W. Cheng, P. W. Huang, M. C. Tsai, and W. H. Lee, "Metal 3D printing of synchronous reluctance motor," in Proceedings of the IEEE International Conference on Industrial Technology, 2016. doi: 10.1109/ICIT.2016.7474912.

[4] J. Krishnasamy and M. Hosek, "Spray-Formed Hybrid-Field Traction Motor," in SAE Technical Papers, 2017. doi: 10.4271/2017-01-1225.

[5] F. N. U. Nishanth, A. D. Goodall, I. Todd, and E. L. Severson, "Characterization of an Axial Flux Machine With an Additively Manufactured Stator," IEEE Transactions on Energy Conversion, vol. 38, no. 4, 2023, doi: 10.1109/TEC.2023.3285539

[6] D. Newman, P. Faue, F. Nishanth, B. Rankouhi, F. E. Pfefferkorn, D. J. Thoma, and E. Severson, "Solid high-speed synchronous reluctance rotor enabled by multi-material additive manufacturing," in *Proc. IEEE Energy Conversion Congress and Exposition (ECCE)*, 2023

[7] Paul C. Krause; Oleg Wasynczuk; Scott D. Sudhoff, "Synchronous Machines," in *Analysis of Electric Machinery and Drive Systems* , IEEE, 2002, pp.191-259, doi: 10.1109/9780470544167.ch5.

[8] M. Schubert and B. Ponick, "Reduction of Eddy Current Losses in Additively Manufactured Synchronous Reluctance Rotors," 2024 International Symposium on Power Electronics, Electrical Drives, Automation and Motion (SPEEDAM), Napoli, Italy, 2024, pp. 1309-1315, doi: 10.1109/SPEEDAM61530.2024.10609070.